

Search for Large Extra Dimensions via Single Photon plus Missing Energy Final States at $\sqrt{s} = 1.96$ TeV

The DØ Collaboration
URL <http://www-d0.fnal.gov>
(Dated: July 22, 2008)

In this note we investigate Kaluza-Klein graviton production with a photon and missing energy in the final state and set limits on the fundamental Planck scale M_D for a set of data with a total integrated luminosity of 2.7 fb^{-1} . At 95% C.L. we set limits on the fundamental mass scale M_D from 970 GeV to 816 GeV for two to eight extra dimensions.

Preliminary Results for Summer 2008 Conferences

I. INTRODUCTION

This note constitutes an update for the analysis described in [1] where we used 1.05 fb^{-1} of data, collected with the $D\bar{O}$ detector [2] at the Fermilab Tevatron collider, to search for LED in the final state with a single photon plus missing transverse energy ($\gamma + \cancel{E}_T$). This signature arises from the process $q\bar{q} \rightarrow \gamma G_{KK}$ (see Fig. 1), which is studied in detail in [3].

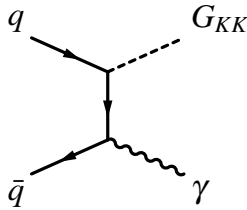


FIG. 1: Feynman diagram for the $q\bar{q} \rightarrow \gamma G_{KK}$ process. Direct graviton production in the $\gamma + \cancel{E}_T$ channel.

In our previous analysis, we derived the following lower limits on M_D at the 95% C.L.: $M_D > 884, 864, 836, 820, 797, 797$ and 778 GeV for $n = 2, 3, 4, 5, 6, 7$ and 8 extra dimensions, respectively. In this study we use the same analysis techniques on 1.7 fb^{-1} [4] of new data. At the end, we present the final results as a combination of both analyses (2.7 fb^{-1} of data).

The selection criteria remains the same as for the analysis in [1], but incorporates a few upgrades due mainly to the higher instantaneous luminosity. The data in this analysis were recorded using triggers requiring at least one energy cluster in the EM section of the calorimeter with transverse momentum $p_T > 20$ GeV. The triggers are almost 100% efficient to select signal events.

The CDF collaboration has recently carried out a similar search with 2 fb^{-1} of data, setting 95% C.L. lower limits on M_D from 1080 GeV to 900 GeV for two to six extra dimensions [5]. Searches for LED in other final states have been performed by collaborations at the Tevatron [6, 7] and the CERN LEP collider [8].

II. EVENT SELECTION

We identify a reconstructed calorimeter cluster as a photon when it satisfies the following requirements: (i) at least 90% of the energy is deposited in the EM section of the calorimeter; (ii) the calorimeter isolation variable $\mathcal{I} = [E_{\text{tot}}(0.4) - E_{\text{em}}(0.2)]/E_{\text{em}}(0.2)$ is less than 0.07, where $E_{\text{tot}}(0.4)$ denotes the total energy deposited in the calorimeter in a cone of radius $\mathcal{R} = \sqrt{(\Delta\eta)^2 + (\Delta\phi)^2} = 0.4$, and $E_{\text{em}}(0.2)$ is the EM energy in a cone of radius $\mathcal{R} = 0.2$. (The cluster fractional isolation has been improved to take into account high luminosity effects); (iii) the track isolation variable, defined as the scalar sum of the transverse momenta of all tracks that originate from the interaction vertex in an annulus of $0.05 < \mathcal{R} < 0.4$ around the cluster, is less than 2 GeV; (iv) it has $|\eta| < 1.1$; (v) both transverse and longitudinal shower shapes are consistent with those of a photon; (vi) it has neither an associated track in the central tracking system nor a significant density of hits in the SMT and CFT systems consistent with the presence of a track with p_T in agreement with its transverse energy; and (vii) there is an energy deposit in the CPS matched to it.

Jets are reconstructed using the iterative midpoint cone algorithm [9] with a cone size of 0.5. The missing transverse energy is computed from calorimeter cells with $|\eta| < 4$ and corrected for the EM and jet energy scales.

The *photon* sample is obtained by selecting events with only one photon with $p_T > 90$ GeV, at least one reconstructed interaction vertex consistent with the measured direction of the photon (see below), and $\cancel{E}_T > 70$ GeV. Additionally, in order to avoid large \cancel{E}_T due to mismeasurement of jet energy, we require no jets with $p_T > 15$ GeV. The applied \cancel{E}_T requirement guarantees negligible multijet background in the final candidate sample while being almost fully efficient for signal selection.

We reject events with reconstructed muons and with cosmic ray muons identified using the timing of the signal in the muon scintillation counters or by the presence of a characteristic pattern of hits in the muon drift chambers that is aligned with the reconstructed photon. In order to further reject events with leptons that leave a distinguishable signature in the tracker but that are not reconstructed in the other subsystems of the detector, we impose a requirement on the p_T of any isolated track not to be greater than 8 GeV. A track is considered to be isolated if the ratio between the scalar sum of the transverse momenta of all tracks that originate from the interaction vertex in an annulus of $0.1 < \mathcal{R} < 0.4$ around the track and the p_T of the track is less than 0.9.

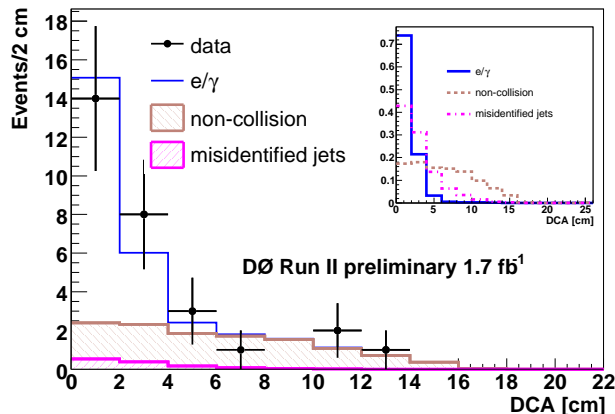


FIG. 2: DCA distribution for the selected events in data (points with statistical uncertainties). The different histograms represent the estimated background composition from the template fit to this distribution. The inset figure compares the individual template shapes.

III. DATA ANALYSIS

The EM pointing algorithm allows calculation of the direction of the EM shower based on the transverse and longitudinal segmentation of the calorimeter and preshower systems. EM pointing is performed independently in the azimuthal and polar planes. The former results in the measurement of the distance of closest approach (DCA) to the z axis (along the beam line), and the latter in the prediction of the z position of the interaction vertex in the event, with a resolution of about 3 cm. We require that the z coordinate of at least one interaction vertex in the event be within 10 cm of the position predicted by the pointing algorithm and use the DCA to estimate the remaining background from jet-photon misidentification and non-collision events. Misidentified jets have poor pointing resolution, and therefore a wider DCA distribution compared to electrons or photons. Likewise, one can anticipate the DCA distribution for photon candidates in non-collision events to have an even wider shape. After these requirements, 29 events are selected in the *photon* sample.

We prepare three DCA distribution templates: the *non-collision* template, the *misidentified jets* template, and the e/γ template. The first template is obtained from a sample in which a photon candidate, passing the same quality requirements as for the *photon* sample, is selected from events with no hard scatter (no reconstructed interaction vertex or fewer than three reconstructed tracks), or from events with identified cosmic muons. The *misidentified jets* template is extracted from the *fake photon* sample, which fulfills exactly the same requirements as the *photon* sample except that the photon track isolation requirement is inverted. This sample is dominated by misidentified jets. Finally, the e/γ template is obtained from a data sample of isolated electrons. The inset in Fig. 2 shows the differences between shapes.

The total number of background events from misidentified jets (N_{misid}) can be predicted from the *fake photon* sample based on the rates at which jets, passing all other photon identification criteria, fail or pass the track isolation requirement. To measure those rates we use an *EM plus jet* sample, where the EM object passes all photon identification requirements except the track isolation, and where the jet approximately balances the EM object in the transverse plane. We first determine the number of events (N_1) in the sample that fail the track isolation requirement; then we fit the DCA distribution of the events that pass the track isolation to a linear sum of the e/γ and *misidentified jets* templates in order to extract the number of misidentified jets (N_2) passing the track isolation. N_{misid} is then equal to the number of events in the *fake photon* sample multiplied by N_2/N_1 . We fit the DCA distribution in the *photon* sample to a linear sum of the three templates, fixing the contribution of *misidentified jets* as described above, and determine the e/γ and *non-collision* contributions. The result of the fit is illustrated in Fig. 2. Most of the signal photons have DCA less than 4 cm, therefore we limit our analysis to this particular window, which contains 22 data events.

The only physics background to the $\gamma + \cancel{E}_T$ final state is the process $Z + \gamma \rightarrow \nu\bar{\nu} + \gamma$. This irreducible contribution is estimated from a sample of MC events generated with PYTHIA [10] using CTEQ6L1 parton distribution functions (PDFs) [11]. The main instrumental background arises from $W \rightarrow e\nu$ decays, where the electron, due to tracking inefficiency or hard bremsstrahlung, is misidentified as a photon. This contribution is estimated from data using a sample of isolated electrons. The same requirements as for the *photon* sample are imposed, and the remaining

TABLE I: Data and estimated backgrounds

Background	Number of expected events (1.7 fb^{-1})	Number of expected events (combined analysis. 2.7 fb^{-1})
$Z + \gamma \rightarrow \nu\bar{\nu} + \gamma$	17.4 ± 2.2	29.5 ± 2.5
$W \rightarrow e\nu$	4.7 ± 1.7	8.5 ± 1.7
Non-collision	3.8 ± 1.8	6.6 ± 2.3
Misidentified jets	0.91 ± 0.23	3.1 ± 1.5
$W + \gamma$	0.72 ± 0.15	2.22 ± 0.3
Total Background	27.5 ± 3.3	49.9 ± 4.1
Data	22	51

number of events is scaled by $(1 - \epsilon_{\text{trk}})/\epsilon_{\text{trk}}$, where ϵ_{trk} is the track reconstruction efficiency of $(98.0 \pm 0.1)\%$. A smaller instrumental contribution to the background is expected from $W + \gamma$ production where the charged lepton in a leptonic W boson decay is not detected; it is estimated using events generated with PYTHIA. We generate signal events [12] with $M_D = 1.5 \text{ TeV}$ for $n = 2, 3, 4, 5, 6, 7$ and 8. For different values of M_D , the cross section scales as $1/M_D^{n+2}$, leaving the kinematic spectra unaffected for a fixed number of extra dimensions.

All MC events are passed through a detector simulation based on the GEANT [13] package, processed using the same reconstruction software as for the data, and corrected for luminosity profile differences with data. Additionally, we apply scale factors, with values ranging from 94% to 98%, to account for the differences between the efficiency determinations from data and simulation.

The main sources of systematic uncertainty are the uncertainty in the photon identification efficiency (5%), the uncertainty in the total integrated luminosity (6.1%), and the uncertainty in the signal acceptance from the PDFs (4%).

For the SM backgrounds estimated from MC, the quoted uncertainties include the uncertainty in the theoretical cross section, which is dominated by the uncertainty in the next-to-leading-order K factors (7%). For the range of p_T in question and for the selection requirements used in this analysis, the K factors vary around unity within this uncertainty margin [14, 15]. The uncertainty in the width of the e/γ sample DCA template results in an additional systematic uncertainty of 0.5 events in the non-collision background estimate.

The final numbers of events for data and backgrounds are given in Table I. Fig. 3 (left) shows the photon p_T distribution, with the SM backgrounds stacked on top of each other.

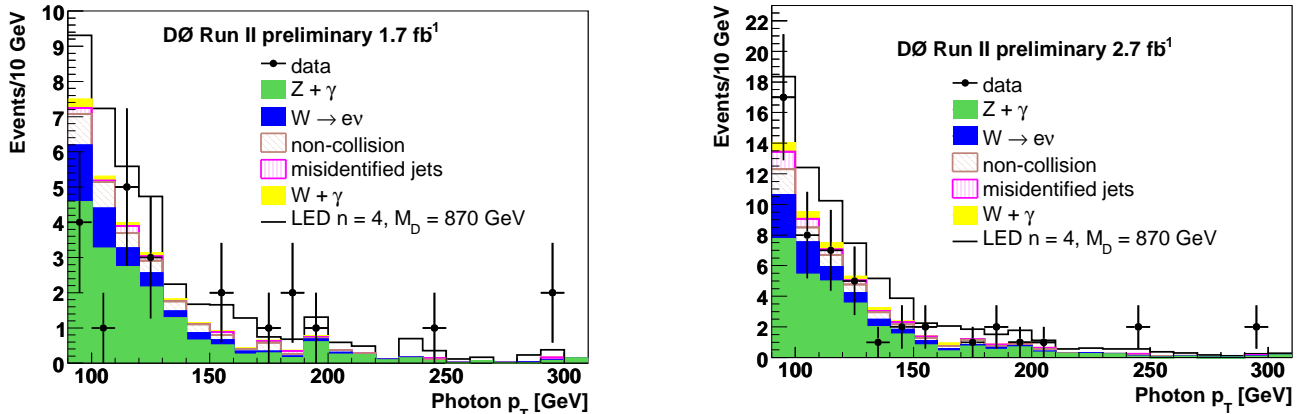


FIG. 3: Photon p_T distribution for the final candidate events with 1.7 fb^{-1} (left) and with 2.7 fb^{-1} (right) after all the selection requirements. Data points show statistical uncertainties. The LED signal is stacked on top of SM backgrounds.

The total efficiency for the MC signal sample is 0.38 ± 0.04 , and it is calculated by applying the same cuts as for our photon sample, and by using the data/MC scale factors in the same way as for the SM backgrounds from MC. There is a drop in efficiency of about 10% compared to our previous analysis where the total efficiency averaged 0.48 ± 0.04 . The main sources of higher inefficiency are a lower efficiency, of about 10%, for matching a CPS energy deposit to the photon, and the jet veto, which contributes a reduction in efficiency of about 12%, measured with MC signal events.

Table I shows the combined final numbers of events with 2.7 fb^{-1} (combination of the present analysis and the one in [1]), for both data and background. We proceed to set limits on the fundamental Planck scale M_D .

Systematic uncertainties between the analysis described in this note and in [1] are very close, but the largest of the two are used in the limit setting procedure. In order to combine the total efficiencies, we perform a luminosity-weighted average of the two values and add an extra systematic uncertainty of 5%. The combined efficiency is then 0.43 ± 0.05 . Fig. 3 (right) shows the photon p_T distribution for the combined analysis, with the SM backgrounds stacked on top of each other. We employ the modified frequentist approach [16] to set limits on the production cross section for the signal. This method is based on a log-likelihood ratio test statistic and uses the binned photon p_T distribution. Assuming the leading-order theoretical cross section for the signal, we derive the following lower limits on M_D at the 95% C.L.: $M_D > 970, 899, 867, 848, 831, 834$ and 804 GeV for $n = 2, 3, 4, 5, 6, 7$ and 8 extra dimensions, respectively. Table II and Fig. 4 summarize the limit setting results.

TABLE II: Summary of limit calculations.

n	1 fb ⁻¹ [1]	1 fb ⁻¹ [1]	2.7 fb ⁻¹	2.7 fb ⁻¹	CDF 2 fb ⁻¹ [5]
	observed (expected) cross section limit (fb)	observed (expected) M_D lower limit (GeV)	observed (expected) cross section limit (fb)	observed (expected) M_D lower limit (GeV)	
2	27.6 (23.4)	884 (921)	19.0 (14.6)	970 (1037)	1080
3	24.5 (22.7)	864 (877)	20.1 (14.7)	899 (957)	1000
4	25.0 (22.8)	836 (848)	20.1 (14.9)	867 (916)	970
5	25.0 (24.8)	820 (821)	19.9 (15.0)	848 (883)	930
6	25.4 (22.3)	797 (810)	18.2 (15.2)	831 (850)	900
7	24.0 (23.1)	797 (801)	15.9 (14.9)	834 (841)	--
8	24.2 (21.9)	778 (786)	17.3 (15.0)	804 (816)	--

To conclude, we have conducted an update to [1] on a search for LED in the $\gamma + \cancel{E}_T$ channel, finding no evidence for their presence. The updated limits show significant improvement from our previous study.

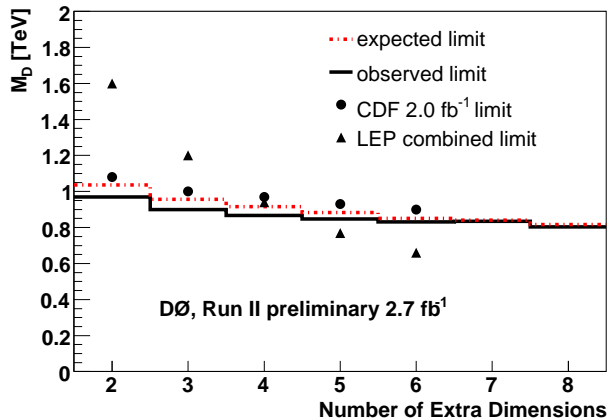


FIG. 4: Expected and observed lower limits on M_D for LED in the $\gamma + \cancel{E}_T$ final state. CDF limits with 2 fb⁻¹ of data (monophoton channel) [5], and the LEP combined limits [8] are also shown.

-
- [1] V.M Abazov *et al.* (D0 Collaboration), Phys. Rev. Lett. **101**, 011601 (2008).
[2] V.M. Abazov *et al.* (D0 Collaboration), Nucl. Instrum. Methods Phys. Res. A **565**, 463 (2006).
[3] G. Guidice, R. Rattazzi, and J. Wells, Nucl. Phys. **B544**, 3 (1999).
[4] T. Andeen *et al.*, FERMILAB-TM-2365 (2007).
[5] T. Aaltonen *et al.* (CDF Collaboration), arXiv:0807.3132v1[hep-ex] (2008)
[6] B. Abbott *et al.* (D0 Collaboration), Phys. Rev. Lett. **86**, 1156 (2001); *ibid* **90**, 251802 (2003); *ibid* **95**, 161602 (2005).
[7] D. Acosta *et al.* (CDF Collaboration), Phys. Rev. Lett. **97**, 171802 (2006).
[8] LEP Exotica Working Group, URL: http://lepexotica.web.cern.ch/LEPEXOTICA/notes/2004-03/ed_note_final.ps.gz, and references therein.
[9] G. C. Blazey *et al.*, arXiv:hep-ex/0005012 (2000).

- [10] T. Sjöstrand *et al.*, *Comput. Phys. Commun.* **135**, 238 (2001).
- [11] J. Pumplin *et al.*, *JHEP* **0207**, 012 (2002); D. Stump *et al.*, *JHEP* **0310**, 046 (2003).
- [12] Stephen Mrenna, private communication.
- [13] R. Brun and F. Carminati, CERN Program Library Long Writeup W5013, 1994.
- [14] U. Baur and E.L. Berger, *Phys. Rev. D* **41**, 1476 (1990).
- [15] U. Baur, T. Han, and J. Ohnemus, *Phys. Rev D* **57**, 2823 (1998).
- [16] W. Fisher, FERMILAB-TM-2386-E (2007); T. Junk, *Nucl. Instrum. Methods Phys. Res. A* **434**, 435 (1999); A. Read, CERN 2000-005 (2000).